ACS APPLIED MATERIALS & INTERFACES

Research Article

www.acsami.org

Ultraflexible Transparent Film Heater Made of Ag Nanowire/PVA Composite for Rapid-Response Thermotherapy Pads

Wei Lan,*[,†,‡,#] Youxin Chen,[†,#] Zhiwei Yang,[†] Weihua Han,[†] Jinyuan Zhou,[†] Yue Zhang,[†] Junya Wang,[†] Guomei Tang,[†] Yupeng Wei,[†,‡] Wei Dou,[§] Qing Su,[†] and Erqing Xie[†]

[†]Key Laboratory of Special Function Materials and Structure Design, Ministry of Education, School of Physical Science and Technology and [§]College of Chemistry and Chemical Engineering, Lanzhou University, 730000 Lanzhou, People's Republic of China

[‡]State Key Laboratory of Advanced Processing and Recycling of Non-ferrous Metals, Lanzhou University of Technology, 730050 Lanzhou, People's Republic of China

Supporting Information

ABSTRACT: Ultraflexible transparent film heaters have been fabricated by embedding conductive silver (Ag) nanowires into a thin poly(vinyl alcohol) film (AgNW/PVA). A cold-pressing method was used to rationally adjust the sheet resistance of the composite films and thus the heating powers of the AgNW/PVA film heaters at certain biases. The film heaters have a favorable optical transmittance (93.1% at 26 Ω/sq) and an outstanding mechanical flexibility (no visible change in sheet resistance after 10 000 bending cycles and at a radius of curvature ≤1 mm). The film heaters have an environmental endurance, and there is no significant performance degradation after being kept at high temperature (80 °C) and high humidity (45 °C, 80% humidity) for half a year. The efficient Joule heating can increase the temperature of the film heaters (20 Ω/sq) to 74 °C in ∼20 s at a bias of 5 V. The fast-heating characteristics at low voltages (a few volts) associated with its transparent and flexibility properties make the poly(dimethylsiloxane)/AgNW/PVA composite film a potential candidate in medical thermotherapy pads.

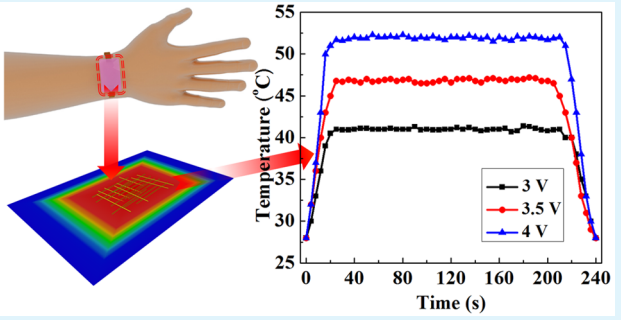

KEYWORDS: *AgNW/PVA film heater, cold pressing, transparent, ultraflexible, thermotherapy pad, thermal response, environmental endurance*

INTRODUCTION

Medical thermotherapy pads (TTPs) are widely used to improve blood circulation, prevent inflammation, and alleviate pains in human bodies, which is one of the classic physiotherapies applied in orthopedics.[1−3] In clinical applications, medical TTPs have been used to treat rheumatic arthritis,[4] scapulohumeral periarthritis,[5] cervical spondylosis,[6] and traumatic injuries.[4] Conventional commercial TTPs are composed of a heating component and a far-infrared paste. These pads often suffer from two main issues, which limits their practical applications. One is the uncontrollable temperature, and the other one is that they have opacity. We cannot see the treatment effect without removing the pads and adjusting the local temperatures according to the conditions.

Recently, a prototype of transparent TTPs had been realized in lab by using transparent conductive films (TCFs) as heaters.[7] On the basis of the stable and controllable Joule heating effect, transparent film heaters (TFHs) can be used as heating components in the TTPs. The performance of the TFHs, such as thermal response time, operating temperature, operating voltage, and cycling stability, mainly depended on the characteristics of TCFs.[8−12] Lee et al.[13] demonstrated a transparent conductive graphene oxide/Ag nanowire (AgNW) film heater with a rising time of 200−600 s under a bias of 12 V. Zhang et al.[14] also fabricated graphene oxide protected AgNW films for the heater and shortened the rising time to 100 s. Furthermore, Kim et al.[15] used AgNW/clay film as heaters on polyethylene terephthalate (PET), which could work at various biases with ∼50 s heating time. Despite the progress achieved on transparency and thermal response time, these film heaters still cannot meet the requirements as transparent TTPs with rapid response. Moreover, the conventional TFHs' flexibility was also insufficient, which hindered further applications due to the insufficient contact to the skin, especially at the joints. More recently, Choi et al.[7] developed an articular transparent TTP based on AgNW/thermoplastic elastomer heater by using patterned poly(dimethylsiloxane) (PDMS) mold, and they found that the heat transfer to muscles or blood vessels was effective and fast. However, the strategy often failed for scale product as well as high cost, and the heating wires were easy to break during bending. Therefore, it is necessary to develop a new strategy for the fabrication of ultraflexible transparent

Received: December 31, 2016
Accepted: February 2, 2017
Published: February 2, 2017

DOI: 10.1021/acsami.6b16853
ACS Appl. Mater. Interfaces 2017, 9, 6644−6651

TTPs with controllable temperatures and rapid thermal response.

Because of the low resistance, high transparency, good mechanical flexibility, and high thermal stability, AgNW networks have been widely used as transparent film heaters.[16−18] The heating power and transparency can be modulated by adjusting the distribution density of the Ag nanowires. However, there are three technical challenges that remained in the use of AgNW networks as TFHs: (1) AgNWs are easily oxidized in air, leading to a high sheet resistance; (2) AgNW networks are readily detached from substrates because of the weak adhesive forces; (3) the high junction resistances between AgNWs lead to high sheet resistances in TCFs. These issues should be addressed before practical applications of AgNWs in TCFs.

In this work, we propose a scalable strategy to fabricate ultraflexible TCFs with AgNW-embedded poly(vinyl alcohol) (PVA) composite films for transparent TTPs. A cold-pressing technique was used to rationally decrease the junction resistance between the AgNWs. PVA was selected to embed and protect the AgNWs, because PVA could be made into a film without high-temperature treatment procedures and it had a high optical transparency. The sheet resistance and optical transmittance of the AgNW/PVA films were modulated by controlling the distribution density of the AgNWs. The AgNW/PVA films were very stable under multiple harsh conditions, such as bending, compressing, and heating, and displayed a good electromechanical flexibility. They showed a great potential in medical transparent and ultraflexible TTPs with rapid thermal response.

EXPERIMENTAL SECTION

Materials. The AgNWs were synthesized via a solution-phase polyol method.[19] Polyvinylpyrrolidone (PVP) and PVA were purchased from Alfa Aesar. Silver nitrate (Aladdin) was used as the Ag source. A 10 wt % aqueous PVA solution was stirred at 60 °C for 24 h. A polyethylene terephthalate (PET) film was used as the substrate. Sylgard 184, which is the monomer of PDMS, was purchased from the Dow Corning Corporation.

Preparation of the AgNW/PVA TCFs. A schematic diagram of the preparation process for the AgNW/PVA films is shown in Figure 1. First, a dispersion of AgNWs was spin-coated onto a cleaned PET substrate and dried at 120 °C for 5 min. The dried AgNW films were then subjected to a pressure of 25 MPa for 30 s and covered with PVA aqueous solution (10 wt %) by drop-coating. The PVA aqueous solution was obtained by dissolved PVA powders into deionized water and stirred at 60 °C for 24 h. The AgNW/PVA films were finally cured at 80 °C for 3 h and peeled from the PET substrates.

Fabrication of the AgNW/PVA TFHs. Electrical contact to the as-prepared AgNW/PVA films was made with copper tape on the films' two terminal sides. The copper tape acted as a bonding material and as an electrode. During deicing processes, the film heater was attached to the back of a glass slide. A direct-current (DC) power supply was used to power the copper electrodes. The deicing demonstration was conducted at an ambient temperature of 5 °C.

Fabrication of the PDMS/AgNW/PVA Transparent TTPs. Two copper (Cu) tapes were attached onto the AgNW/PVA films as electrodes. The AgNW/PVA film and the Cu electrodes were covered with a layer of PDMS, which was subsequently cured at 65 °C for 3 h for the curing of the PDMS. A tip of the Cu tape was exposed for the connection of the power supply. After fabrication of the PDMS/AgNW/PVA thermotherapy pad, a DC power supply was used to perform thermal therapy.

Characterization. The morphologies of the AgNW/PVA films were investigated by field emission scanning electron microscopy (FE-SEM, Hitachi S-4800). The sheet resistance was measured with a four-point probe technique. Real-time resistance was measured using a digital multimeter (Keysight 2700). Optical transmission spectra were measured with a Hitachi spectro-photometer (U-3900). Atomic force microscopy (AFM, Asylum Cypher) was performed on an Asylum Cypher under ambient conditions. Bending tests were performed using a bending device (SHSIWI SJH-500). The biases were applied to the two copper electrodes using a DC power supply (RD-3030, SuZhou Varied Electronics). A digital multimeter was used to measure the average surface temperature of the transparent film heaters in real time via a thermocouple. An infrared radiation thermometer was used to monitor the surface temperature of the transparent thermotherapy pad. Infrared photographs and videos of the transparent film heaters were taken during heating with an infrared camera (FLIR T460).

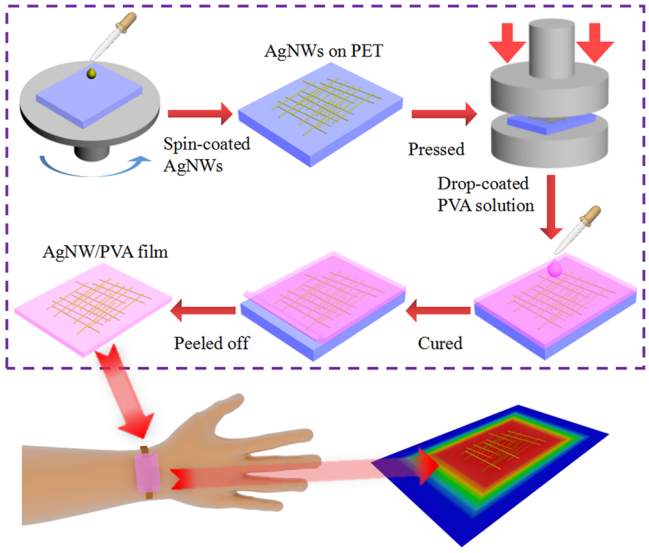

Figure 1. Schematic diagram of the procedure used to fabricate ultraflexible AgNW/PVA TCFs.

RESULTS AND DISCUSSION

The electrical resistances of the AgNW films are derived from those of the individual AgNWs and the junctions between the AgNWs. Generally, reducing the junction resistance is one of the effective ways to improve the electrical conductivity of AgNW films.[20] Longer and thinner AgNWs are preferred to achieve TCFs with low resistances and high transmittances. An increased nanowire length will decrease the number of junctions and reduce the overall junction resistance. Using smaller diameter wires increases the duty ratio and enhances light transmittance. Therefore, AgNWs with average diameters of ∼30 nm and aspect ratios of ∼800 were synthesized to prepare the AgNW TCFs.

Figure 1 shows a schematic diagram of the fabrication process of ultraflexible AgNW/PVA TCFs for transparent thermotherapy pads. Benefitting from the weak adhesion of the spin-coated AgNWs and the PET substrates, the drop-coated PVA solution easily penetrated into the gaps between the AgNWs and the PET substrate. The AgNWs were partially encased in the cured PVA films, and it was easy to peel from the PET substrate due to the weak chemical bonding between PVA and PET. As shown in the SEM images (Figure 2), the AgNW films were not damaged after being removed from the PET substrate.

The distribution density of the nanowires in the AgNW/PVA films was controlled by changing the concentrations of AgNWs dispersion and deposition processes. The sheet resistances and optical transmittances of the AgNW/PVA films were closely

DOI: 10.1021/acsami.6b16853
ACS Appl. Mater. Interfaces 2017, 9, 6644−6651

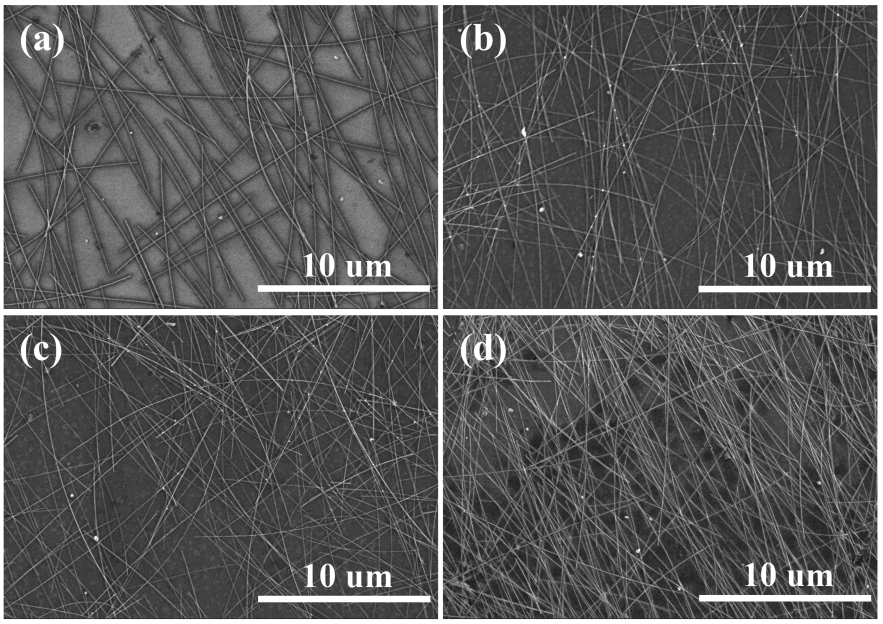

Figure 2. SEM images of AgNW/PVA films with different AgNW distribution densities of (a) 0.37, (b) 0.61, (c) 0.83, and (d) 1.06 μm^{-2}.

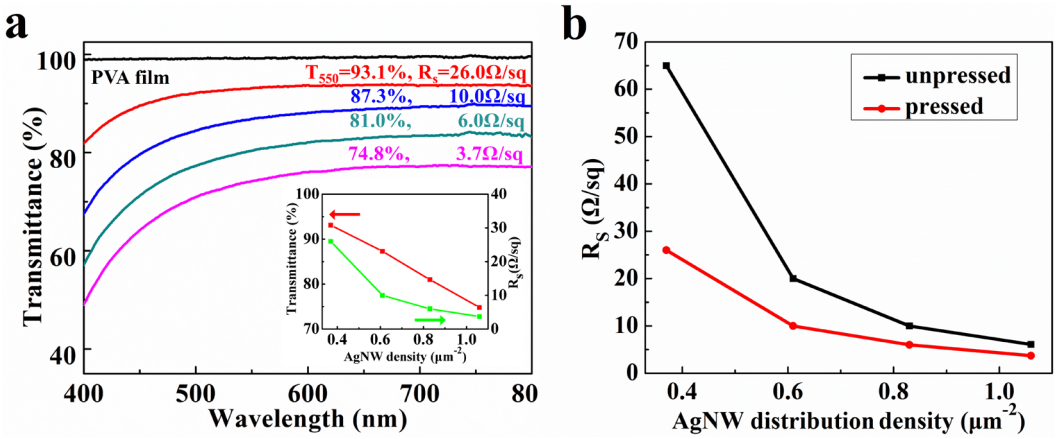

Figure 3. (a) Optical transmittances of the AgNW/PVA films at different sheet resistances. (inset) The dependence of optical transmittance and sheet resistance on the AgNWs distribution density. (b) Sheet resistances of the AgNW/PVA films as a function of AgNW distribution density before and after pressing.

related to the distribution density of AgNWs. Figure 2 shows typical SEM images of AgNW/PVA films with different AgNW distribution densities. The densities ranged from 0.37 to 1.06 μm^{-2}, which was fitted in Figure S1 (Supporting Information). The AgNWs were randomly distributed and embedded in the PVA film forming a conductive network, establishing the junctions between the AgNWs. Even at a lower density of 0.37 μm^{-2}, the AgNWs had formed the high-quality, continuous conductive networks. As the AgNW distribution density increased, more AgNW junctions would be formed, which served as the transfer paths of electrons.

Figure 3a shows the optical transmittance spectra and sheet resistances of the AgNW/PVA films. The optical transmittances at 550 nm and the sheet resistances of the AgNW/PVA films gradually decreased as the AgNW distribution density increased from 0.37 to 1.06 μm^{-2}. These trends were the result of the stronger scattering and reflection of photons and the increase in conductive pathways at high AgNW densities. In addition, the optical transmittances of the AgNW/PVA films had a nearly linear relationship with the AgNW distribution density, as reported previously.[21] At a distribution density of ~0.37 μm^{-2}, the sheet resistances of both the unpressed and the pressed AgNW/PVA films decreased rapidly with increasing AgNW distribution density. At ~0.83 μm^{-2}, the sheet resistance decreased more slowly with increasing AgNW distribution density before reaching a constant value. These relationships can be used to design TCFs with desired characteristics to meet the needs of various applications. Compared with the unpressed AgNW/PVA films, the sheet resistances of the pressed ones were obviously decreased in the whole range of distribution density. Note that the sheet resistances of the pressed AgNW/PVA films were, on average, 47% lower than those of the unpressed films (Figure 3b). This observation verifies that the decreased junction resistance between the AgNWs was mainly caused by the cold pressing process.

AFM images were acquired and analyzed for the unpressed and pressed as-spin-coated AgNW films on PET substrates (Figure S2, Supporting Information). A considerable decrease in the junction height occurred after cold pressing of the AgNW films at 25 MPa for 30 s. The junction height decreased

DOI: 10.1021/acsami.6b16853
ACS Appl. Mater. Interfaces 2017, 9, 6644−6651

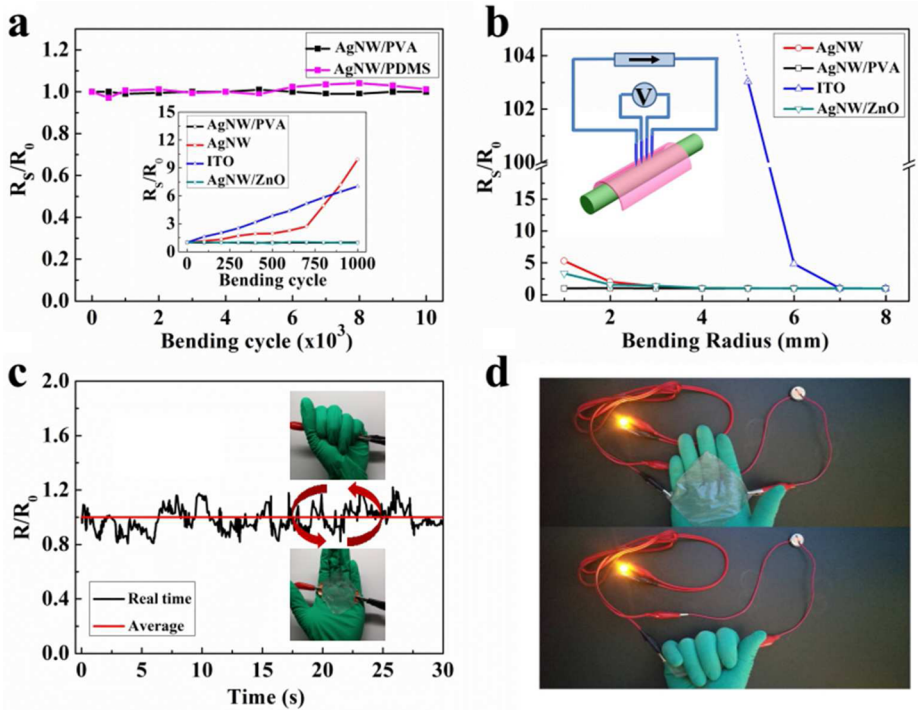

Figure 4. (a) Sheet resistances of a AgNW/PVA film (T_{550} = 87.3%, R_s = 10 Ω/sq) and AgNW/PDMS (T_{550} = 81%, R_s = 10 Ω/sq) as a function of bending cycle. (inset) Sheet resistances of ITO, AgNW, AgNW/ZnO, and AgNW/PVA films. (b) Sheet resistance of ITO, AgNW, AgNW/ZnO,[21] and AgNW/PVA films as a function of bending radius. (c) Real-time resistance of the AgNW/PVA film (T_{550} = 74.8%, R_s = 3.7 Ω/sq) during multiple random compressions. (d) Digital photographs of an 8 cm × 8 cm AgNW/PVA film (T_{550} = 74.8%, R_s = 3.7 Ω/sq) used as a conductor in the circuit before (top) and after (bottom) manual compression.

by 31% after pressing from 65 to 45 nm. The improved contact between the AgNWs caused the resistance decrease of the AgNW/PVA films.

Metallic nanowire networks are promising flexible electrode materials because of their outstanding bending properties.[22−24] To meet the mechanical requirements of flexible electronics, the AgNW/PVA TCFs should be much more flexible than conventional indium tin oxide (ITO) films, which are prone to cracking.[25] The flexibility of the AgNW/PVA TCFs were estimated by periodically bending the films and measuring the change of sheet resistance. The bending radius was at a curvature of 5 mm. Figure 4a shows a comparison of the mechanical flexibilities of ITO, AgNW, AgNW/PVA, and AgNW/ZnO films,[20] as a function of bending cycle. The sheet resistance was measured in the flat mode after being released from bending, as shown in Figure S3a (Supporting Information). After 1000 bending cycles, the sheet resistance of the AgNW/PVA film remained constant, while the sheet resistances of the AgNW and ITO films increased from 22 to 218 Ω/sq (~10 times) and from 36 to 253 Ω/sq (~7 times), respectively. Even after 10 000 bending cycles, the sheet resistance of the AgNW/PVA film still remained constant. Moreover, the flexibility of the AgNW/PVA film was also better than that of the AgNW/PDMS film. In addition, a real-time bending measurement was also performed to further investigate the mechanical flexibilities of the AgNW/PVA films. Figure 4b shows the sheet resistances of the ITO, AgNW, AgNW/ZnO, and AgNW/PVA films as a function of the bending radius. Here, the sheet resistance was measured in a bending mode, as shown in Figure S3b (Supporting Information). The sheet resistance of the AgNW/PVA films was almost the same as free-standing, even bending up to a radius of 1 mm. Because of ITO's brittleness, the sheet resistance of the ITO film increased to 17 kΩ/sq when it was bent to a radius of 4 mm. This sharp increase in sheet resistance indicated that the ITO film had begun to crack. The sheet resistance of an AgNW film on a PET substrate without any coating increased by 5 times at a bending radius of 1 mm, and the sheet resistance of a previously studied AgNW/ZnO film increased by 3 times under the same bending conditions. These observations indicate that the AgNW/PVA films have an outstanding mechanical flexibility.

To further confirm the excellent flexibility of the AgNW/PVA films, real-time resistance measurements were made with a digital multimeter while the film was irregularly compressed by hand. As shown in Figure 4c, the resistance changed by 20% around the initial value during compression. Once the compression was released, the resistance returned to its initial value. In addition, the AgNW/PVA films was used as a conductor in a circuit to light a light-emitting diode (LED; Figure 4d). There was no visible change of the LED brightness when the film was compressed. In addition, a sellotape test on adhering to the AgNW/PVA films revealed that the sheet resistance did not change after sticking many times. These results confirmed that the AgNW/PVA films had an excellent mechanical flexibility that prevented deleterious side effects during bending, such as shedding, fracture, and aggregation.

The AgNW/PVA films can work as a thermal component for potential application as transparent TTPs based on the Joule heating effect, which follows

$$Q = \frac{U^2}{R} \cdot t \quad (1)$$

where Q is the generated Joule, U is the bias voltage, R is the resistance of the AgNW/PVA film, and t is the operating time.

DOI: 10.1021/acsami.6b16853
ACS Appl. Mater. Interfaces 2017, 9, 6644−6651

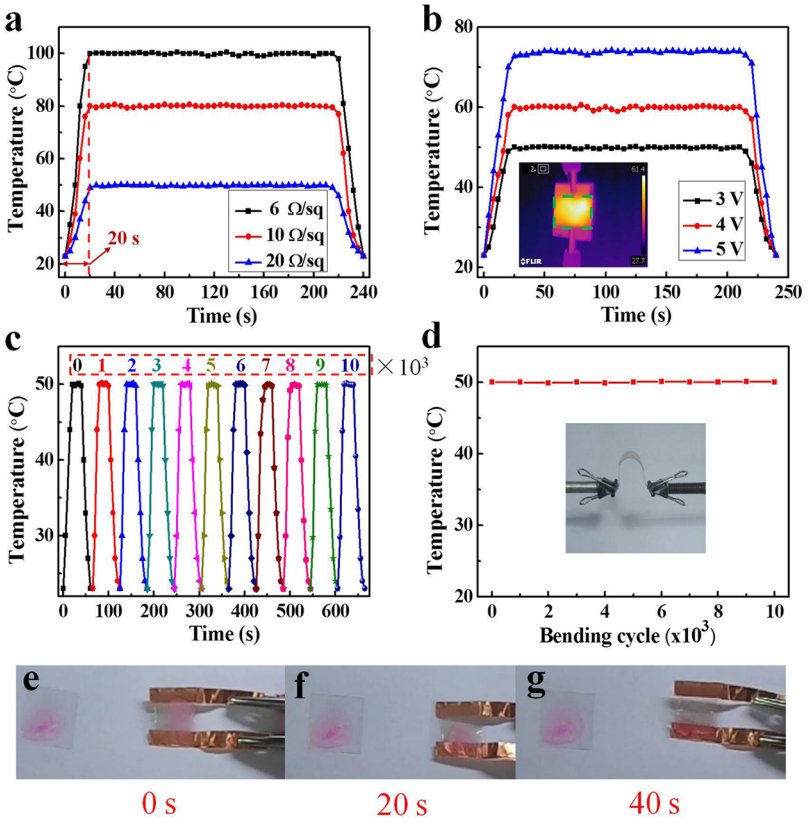

Figure 5. (a) Time-dependent temperature profiles of AgNW/PVA transparent film heaters with different sheet resistances. (b) Temperature profiles of the AgNW/PVA film heater (T_{550} = 90.5%, R_s = 20 Ω/sq) operated at different voltages. (c) Temperature response of the AgNW/PVA film heater over 10 heating cycles. Bending tests (1000) were performed between two heating measurements. (d) Temperature stability of the AgNW/PVA film heater (T_{550} = 90.5%, R_s = 20 Ω/sq) during 10 000 bending cycles. (e−g) Digital photographs of the deicing process on a glass slide with red ice after 0, 20, and 40 s of heating, respectively.

The heat power is affected by the bias and the resistance of the AgNW/PVA film. Figure 5a shows the time-dependent temperature profiles of the AgNW/PVA film heaters with different sheet resistances. The temperature was recorded at the same bias for each the film heaters. Clearly, the temperature increased rapidly and reached its saturation value (operating temperature) within ∼20 s. At the same applied voltage (3 V), the operating temperature was controlled by the sheet resistances of the AgNW/PVA films. For film heaters with the same resistance, a higher voltage resulted in a higher operating temperature (Figure 5b). An operating temperature of 73 °C was obtained on the film heater with R_s = 20 Ω/sq at V = 5 V. Infrared photography of the film heater at a constant applied voltage (inset to Figure 5b) clearly revealed that the temperature distribution on the film area (green rectangle) was uniform. As shown in the infrared videos and the infrared photographies (Video S1, Figure S4, Supporting Information), the temperature distribution was also uniform for the AgNW/PVA film heaters at different biases.

A long-term stability measurement of typical AgNW/PVA transparent film heaters is shown in Figure 5c. During the cycling tests, the temperature reached the same value when the same bias was applied, and the temperature responses were similar without observable change after unloading. The temperature response time was also stable after bending 1000 times between two heating measurements (Figure 5d). After 10 000 bending cycles, the operating temperature did not change significantly, revealing the high thermal and mechanical stability of the AgNW/PVA film heaters. To demonstrate its potential application, a deicing test was performed on a glass slice with a AgNW/PVA film heater attached to the back of a glass slide. Red ice was frozen in a refrigerator on the front of the glass slide. When the film heater was biased at 3 V, the red ice was completely melted within 40 s at an ambient temperature of 5 °C (Figure 5e−g, Video S2, Supporting Information), while it almost kept the same without the film heater. Therefore, the AgNW/PVA TFHs were also useful for antifogging, deicing, and snow removal from the surfaces of displays, vehicle headlights, traffic lights, windows, camera lenses, and touchscreens.

The PDMS/AgNW/PVA transparent TTPs were fabricated by using the AgNW/PVA films as the heating component. TTPs are usually attached to the skin to increase the local temperature and activate blood circulation. As applied the transparent film heaters, the heating of transparent TTPs should be more gentle. Figure 6a1,a2 shows a schematic diagram and a digital photograph of the demonstrated PDMS/AgNW/PVA TTP. The AgNW/PVA film and copper electrodes were covered by a layer of biocompatible PDMS materials, which was used as an insulator to protect the skin. As seen, the logo of Lanzhou University was very clear through the thermotherapy pad. Figure 6b,c shows the time-dependent temperature profiles of the PDMS/AgNW/PVA TTP at various biases. For biases of 0, 3, 3.5, and 4 V, the operating temperatures of the TTP were ∼29.1, 42.0, 47.0, and 52.1 °C, respectively. Figure 6e−g shows digital photographs of the TTP at applied voltages of 0, 3, and 4 V. The TTP quickly reached its maximum temperature within ∼20 s and remained constant,

DOI: 10.1021/acsami.6b16853
ACS Appl. Mater. Interfaces 2017, 9, 6644−6651

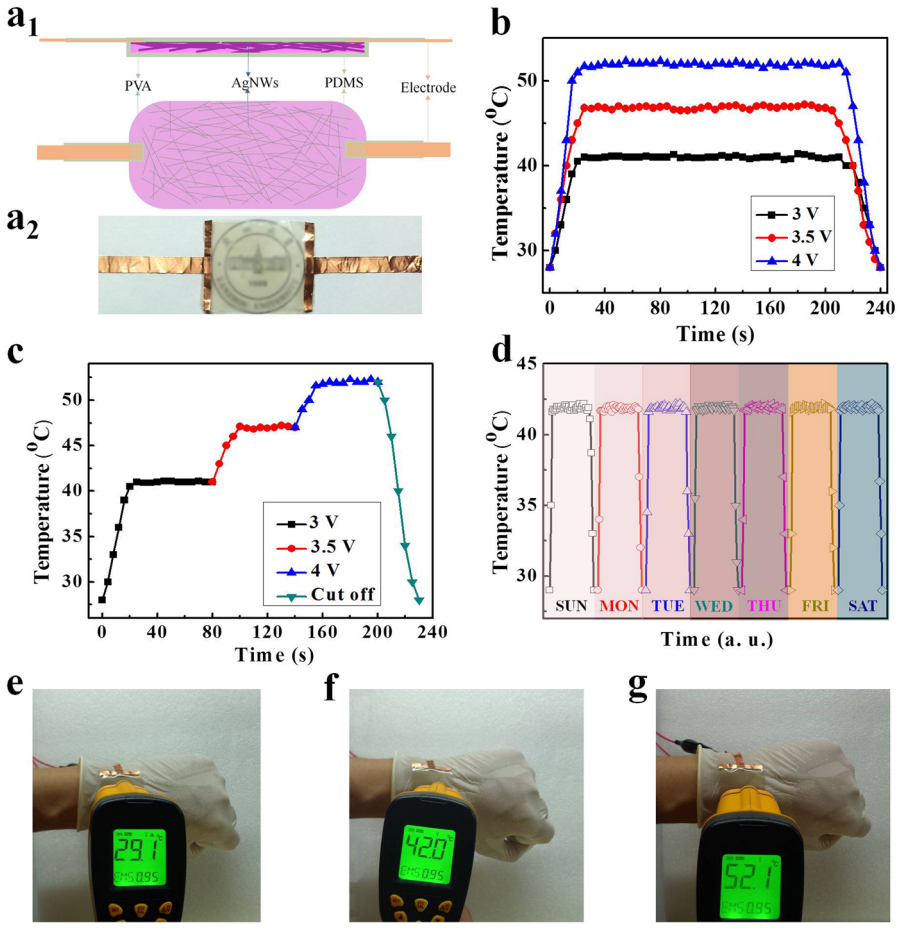

Figure 6. (a1, a2) Schematic diagram and digital photograph of the PDMS/AgNW/PVA thermotherapy pad (T_{550} = 85%, R_s = 20 Ω/sq). (b, c) Temperature profiles of the thermotherapy pad operated at different biases. (d) Temperature response of the thermotherapy pad over seven cycles in a week, each cycle was 20 min long. (e–g) Digital photographs of a thermotherapy pad in use with applied biases of 0, 3, and 4 V, respectively.

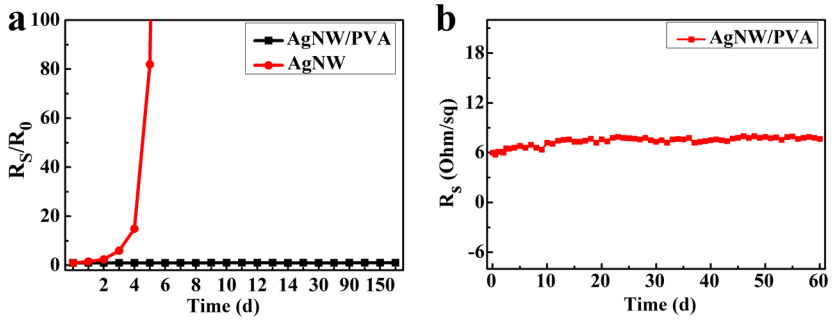

Figure 7. (a) Sheet resistance of the AgNW and AgNW/PVA films (T_{550} = 81%, R_s = 6 Ω/sq) as a function of time (at 80 °C in air). (b) Sheet resistance of the AgNW/PVA films (T_{550} = 81%, R_s = 6 Ω/sq) as a function of time (at 45 °C temperature and 80 ± 10% humidity in air).

which was much faster than the previously reported results.[7−10] During thermotherapy, the patients can obviously feel the temperature increase of the TTP, and the heating effect can be directly observed through the transparent PDMS/AgNW/PVA thermotherapy pad. The actual thermal sensation experienced by the users might be slightly less than that indicated by the operating temperature because of the low thermal conductivity of the PDMS. In addition, as shown in Figure 6d, there was no obvious decrease in the operating temperature and response time at an applied voltage of 3 V for 7 cycles, indicating the good heating stability of these materials. This stability originated from the excellent performance of AgNW/PVA film heaters and the protecting effect of the PDMS layer.

Although the AgNW/PVA film heaters had the favorable transmittance, conductivity and better flexibility, their use as transparent TTPs required an excellent thermal stability and adhesion properties. To determine the long-term thermal stability of the AgNW/PVA film heaters, the AgNW and AgNW/PVA films were held at 80 °C for six months. The sheet resistance of the AgNW/PVA films remained nearly constant over this time (Figure 7a), while the sheet resistance of the AgNW films increased to ∼15 kΩ/sq after 7 d. On the one hand, these results suggested that the PVA layer successfully

DOI: 10.1021/acsami.6b16853
ACS Appl. Mater. Interfaces 2017, 9, 6644−6651

protected the AgNWs from oxidation at high temperatures and maintained the high electrical conductivity of the films. On the other hand, the environment with high temperature and high humidity often exists in some areas. To demonstrate the adaptability of the PDMS/AgNW/PVA TTPs in these environments, a thermal stability of AgNW/PVA films under high-temperature and high-humidity environment was performed. An environment of high humidity and high temperature was simulated in vacuum drying oven; the temperature was 45 °C, and the humidity was adjusted to 80 ± 10% (Figure S5 Supporting Information). As shown in Figure 7b, it was found that the sheet resistance of AgNW/PVA films hardly changed after two months. It is reasonable to believe that after wrapped PDMS layer, the thermal stability of the PDMS/AgNW/PVA TTPs would be much more excellent in harsh environments. As shown in Table S1 (Supporting Information), the performances of the AgNW/PVA TCFs had been compared with other reported results. It was found that the comprehensive performances of the AgNW/PVA TCFs were significantly excellent. Therefore, it was definite that the wearable PDMS/AgNW/PVA TTPs had the simple fabrication process, low cost, high transparency, rapid thermal response, controllable operating temperature, and environmental adaptability, which may have wide potential applications in various fields.

CONCLUSION

A simple strategy was proposed to fabricate high-performance, ultraflexible AgNW/PVA film heaters for transparent thermotherapy pads. The sheet resistances and optical transmittances of the AgNW/PVA films were modulated by changing the distribution density of the AgNWs. The as-prepared AgNW/PVA films exhibited excellent mechanical flexibilities and long-term thermal stabilities, and they were very stable under different harsh conditions. The AgNW/PVA film heaters are good candidates for transparent TTPs. The PDMS/AgNW/PVA TTPs achieved stable, mild, and controllable heating with rapid thermal response, enabling potential applications in the field of medical thermotherapy.

ASSOCIATED CONTENT

Supporting Information

The Supporting Information is available free of charge on the ACS Publications website at DOI: 10.1021/acsami.6b16853.

An infrared video of the AgNW/PVA film heater when the applied voltage was increased from 0 to 3 V (AVI)
A melting process of red ice on glass when the AgNW/PVA film heater was powered at 3 V (AVI)
The fitted patterns of the AgNW distribution density in Figure 2 SEM images. AFM images of (a) the unpressed and (b) the pressed AgNW films. The measurement mode of sheet resistance for the AgNW/PVA films in Figure 4. The infrared photographs of the AgNW/PVA film heater during the heating process at 3 V bias. Digital photographs of vacuum drying oven with high-temperature (45 °C) and high-humidity (80 ± 10%) environment for the AgNW/PVA films. FTIR and Raman patterns of pure PVA films before and after six months. The characterization comparison of AgNW/PVA TCFs with the other nanowire-based TCFs (PDF)

AUTHOR INFORMATION

Corresponding Author

*E-mail: lanw@lzu.edu.cn.

ORCID

Wei Lan: 0000-0001-6194-4839

Author Contributions

#W.L. and Y.C. contributed equally to this work.

Notes

The authors declare no competing financial interest.

ACKNOWLEDGMENTS

This work was supported by Natural Science Foundation of Gansu Province (No. 1208RJZA199), the fund of the State Key Laboratory of Advanced Processing and Recycling of Nonferrous Metals, Lanzhou University of Technology (SKLAB02014003), and the Project-sponsored by SRF for ROCS, SEM.

REFERENCES

(1) Petrofsky, J. S.; Laymon, M.; Lee, H. Effect of Heat and Cold on Tendon Flexibility and Force to Flex the Human Knee. *Med. Sci. Monit.* **2013**, *19*, 661−667.
(2) Brosseau, L.; Yonge, K. A.; Welch, V.; Marchand, S.; Judd, M.; Wells, G.; Tugwell, P. Thermotherapy for Treatment of Osteoarthritis. *Cochrane Database Syst. Rev.* **2003**, CD004522.
(3) Michlovitz, S.; Hun, L.; Erasala, G. N.; Hengehold, D. a.; Weingand, K. W. Continuous Low-Level Heat Wrap Therapy Is Effective for Treating Wrist Pain. *Arch. Phys. Med. Rehabil.* **2004**, *85*, 1409−1416.
(4) Nadler, S. F.; Weingand, K.; Kruse, R. J. The Physiologic Basis and Clinical Applications of Cryotherapy and Thermotherapy for The Pain Practitioner. *Pain Physician* **2004**, *7*, 395−400.
(5) Barua, S. K.; Chowdhury, M. Z. A. Phonophoresis in Adhesive Capsulitis (Frozen Shoulder). *Chattagram Maa-O-Shishu Hospital Medical College Journal* **2014**, *13*, 60−64.
(6) Lin, J. H.; Chiu, T. T. W.; Hu, J. Chinese Manipulation for Mechanical Neck Pain: a Systematic Review. Clinical Rehabilitation. *Clin Rehabil* **2012**, *26*, 963−973.
(7) Choi, S.; Park, J.; Hyun, W.; Kim, J.; Kim, J.; Lee, Y. B.; Song, C.; Hwang, H. J.; Kim, J. H.; Hyeon, T.; Kim, D. H. Stretchable Heater Using Ligand-Exchanged Silver Nanowire Nanocomposite for Wearable Articular Thermotherapy. *ACS Nano* **2015**, *9*, 6626−6633.
(8) Hong, S.; Lee, H.; Lee, J.; Kwon, J.; Han, S.; Suh, Y. D.; Cho, H.; Shin, J.; Yeo, J.; Ko, S. H. Highly Stretchable and Transparent Metal Nanowire Heater for Wearable Electronics Applications. *Adv. Mater.* **2015**, *27*, 4744−4751.
(9) Ding, S.; Jiu, J. T.; Gao, Y.; Tian, Y. H.; Araki, T.; Sugahara, T.; Nagao, S.; Nogi, M.; Koga, H.; Suganuma, K.; Uchida, H. One-Step Fabrication of Stretchable Copper Nanowire Conductors by a Fast Photonic Sintering Technique and Its Application in Wearable Devices. *ACS Appl. Mater. Interfaces* **2016**, *8*, 6190−6199.
(10) Jeong, S. M.; Kim, J. H.; Song, S.; Seo, J.; Hong, J. I.; Ha, N. Y.; Takezoe, H.; Jeong, J.; Kim, H. Conductive, Flexible Transparent Electrodes Based on Mechanically Rubbed Nonconductive Polymer Containing Silver Nanowires. *RSC Adv.* **2015**, *5*, 51086−51091.
(11) Liu, G. S.; Liu, C.; Chen, H. J.; Cao, W.; Qiu, J. S.; Shieh, H. D.; Yang, B. R. Electrically Robust Silver Nanowire Patterns Transferrable onto Various Substrates. *Nanoscale* **2016**, *8*, 5507−5515.
(12) Tian, J. L.; Zhang, H. Y.; Wang, H. J. Preparation and Properties of Silver Nanowire-Based Transparent Conductive Composite Films. *J. Electron. Mater.* **2016**, *45*, 3040−3045.
(13) Lee, S. M.; Lee, J. H.; Bak, S.; Lee, K.; Li, Y.; Lee, H. Hybrid Windshield-Glass Heater for Commercial Vehicles Fabricated via Enhanced Electrostatic Interactions among a Substrate, Silver nanowires, and an Over-Coating Layer. *Nano Res.* **2015**, *8* (6), 1882−1892.

DOI: 10.1021/acsami.6b16853
ACS Appl. Mater. Interfaces 2017, 9, 6644−6651

(14) Zhang, X.; Yan, X. B.; Chen, J. T.; Zhao, J. P. Large-Size Graphene Microsheets as a Protective Layer for Transparent Conductive Silver Nanowire Film-Heaters. *Carbon* **2014**, *69*, 437−443.
(15) Kim, T. Y.; Kim, Y. W.; Lee, H. S.; Kim, H.; Yang, W. S.; Suh, K. S. Uniformly Interconnected Silver-Nanowire Networks for Transparent Film Heaters. *Adv. Funct. Mater.* **2013**, *23*, 1250−1255.
(16) He, X.; He, R. H.; Liu, A. L.; Chen, X. Y.; Zhao, Z. L.; Feng, S.; Chen, N.; Zhang, M. A Highly Conductive, Flexible, Transparent Composite Electrode Based on the Lamination of Silver Nanowires and Polyvinyl Alcohol. *J. Mater. Chem. C* **2014**, *2*, 9737−9745.
(17) Yoon, S. S.; Khang, D. Y. Facile Patterning of Ag Nanowires Network by Micro-Contact Printing of Siloxane. *ACS Appl. Mater. Interfaces* **2016**, *8*, 23236−23243.
(18) Song, C. H.; Han, C. J.; Ju, B. K.; Kim, J. W. Photoenhanced Patterning of Metal Nanowire Networks for Fabrication of Ultra-flexible Transparent Devices. *ACS Appl. Mater. Interfaces* **2016**, *8*, 480−489.
(19) Ran, Y.; He, W.; Wang, K.; Ji, S.; Ye, C. A One-Step Route to Ag Nanowires with a Diameter Below 40 nm and an Aspect Ratio Above 1000. *Chem. Commun. (Cambridge, U. K.)* **2014**, *50*, 14877−14880.
(20) Bellew, A. T.; Manning, H. G.; Gomes da Rocha, C.; Ferreira, M. S.; Boland, J. J. Resistance of Single Ag Nanowire Junctions and Their Role in the Conductivity of Nanowire Networks. *ACS Nano* **2015**, *9*, 11422−11429.
(21) Chen, Y.; Lan, W.; Wang, J.; Zhu, R.; Yang, Z.; Ding, D.; Tang, G.; Wang, K.; Su, Q.; Xie, E. Highly Flexible, Transparent, Conductive and Antibacterial Films Made of Spin-Coated Silver Nanowires and a Protective ZnO Layer. *Phys. E (Amsterdam, Neth.)* **2016**, *76*, 88−94.
(22) De, S.; Higgins, T. M.; Lyons, P. E.; Doherty, E. M.; Nirmalraj, P. N.; Blau, W. J.; Boland, J. J.; Coleman, J. N. Silver Nanowire Networks as Flexible, Transparent, Conducting Films: Extremely High DC to Optical Conductivity Ratios. *ACS Nano* **2009**, *3*, 1767−1774.
(23) Rathmell, A. R.; Bergin, S. M.; Hua, Y.-L.; Li, Z.-Y.; Wiley, B. J. The Growth Mechanism of Copper Nanowires and Their Properties in Flexible, Transparent Conducting Films. *Adv. Mater.* **2010**, *22*, 3558−3563.
(24) Madaria, A. R.; Kumar, A.; Ishikawa, F. N.; Zhou, C. Uniform, Highly Conductive, and Patterned Transparent Films of a Percolating Silver Nanowire Network on Rigid and Flexible Substrate Using a Dry Transfer Technique. *Nano Res.* **2010**, *3*, 564−573.
(25) Alzoubi, K.; Hamasha, M. M.; Lu, S.; Sammakia, B. Bending Fatigue Study of Sputtered ITO on Flexible Substrate. *J. Disp. Technol.* **2011**, *7*, 593−600.

DOI: 10.1021/acsami.6b16853
ACS Appl. Mater. Interfaces 2017, 9, 6644−6651